December 2009 *Volume 4 Issue 2*

Trade Science Inc.

Physical CHEMISTRY
An Indian Journal

Full Paper

PCAIJ, 4(2), 2009 [65-70]

AC electrical properties study and equivalent circuit of a monovalent mixed pyrophosphate

M.Megdiche*, H.Mahmoud, B.Louati, F.Hlel, K.Guidara
Laboratoire de L'Etat Solide, Faculté des Sciences de Sfax-3031, Sfax, (TUNISIA)
E-mail : m_megdiche@yahoo.fr
Received: 17th December, 2009 ; Accepted: 27th December, 2009

ABSTRACT

$NaAgPbP_2O_7$ was prepared with a solid state reaction. The electrical properties were investigated by using impedance measurements in the frequency range from 200Hz to 5MHz with the TEGAM 3550 ALF automatic bridge monitored by a microcomputer between 581K and 703K. The Z′ and Z″ versus frequency plots are well fitted to an equivalent circuit model. The conductivity data obey the universal power law. The conductivity in the material is due to the hopping of monovalent ions parallel to (001) plane.

KEYWORDS

AC conductivity;
Equivalent circuit;
Pyrophosphate;
$NaAgPbP_2O_7$.

INTRODUCTION

In the recent years interest for preparation, theoretical and experimental research of phosphate has been increased. The metal phosphates are of considerable industrial interest, which might find applications such as prospective materials in technology, electronic devices and as solid electrolytes with high thermal resistance and as potential devices in space application, sensors, solid-state laser materials, piezoelectrics, ceramics, catalysis, adsorption, ionic conductors and magnetic materials[1-7]. Crystals of double phosphates with general formula $A_2BP_2O_7$ containing simultaneously an alkaline ion (A^+) and a divalent cation (B^{2+}), form a large family of materials[8,9]. In our laboratory we are interested to the partially substituted compounds with chemical formula $Na_{2-x}M_xPbP_2O_7$ (M = Ag, Li, Na, K) in order to discuss the effect of the substitution monovalent on ionic conduction. The structures and ionic conductivity of the $Ag_2PbP_2O_7$ and $Na_2PbP_2O_7$ are comment in the literature[10,11]. The previous results show $Ag_2PbP_2O_7$, isotype of $Na_2PbP_2O_7$, is of triclinic symmetry with the space group $P(\bar{1})$ (Z=2), the unit cell parameters are: a=5.502Å, b=7.008 Å, c=10.018 Å, α=106.63°, β=93.89°, γ=110.68°. The better electrical properties obtained for $Ag_2PbP_2O_7$ can be attributed to the higher polarizability of Ag^+ ions, more easily deformed (d^{10} configuration) to pass through the bottlenecks and consequently more mobile than the Na^+ ions (rare gas type configuration)[10]. In this work, we propose to investigate, structural and electrical properties of the mixed compound corresponding to x = 1, $NaAgPbP_2O_7$.

EXPERIMENTAL METHODS

Synthesis of double phosphate powder of $NaAgPbP_2O_7$ was carried out by conventional solid-state reaction techniques. Stoichiometric quantities of

Na_2CO_3, $AgNO_3$ and $NH_4H_2PO_4$ were well ground, mixed, and progressively heated first to 473K to expel NH_3, H_2O and CO_2, then the powders were pressed into pellets of 8mm diameter and sintered at 873K in air for 4 hours with intermediate regrinding and repelling.

Before electrical measurements the samples were heated at 473K. This treatment is carried to eliminate, as much as possible, the water content in the pellet pores. The ac impedance data were measured in the frequency range from 200Hz to 5MHz with the TEGAM 3550 ALF automatic bridge monitored by a microcomputer between 581K and 703K.

X-ray powder diffraction pattern was recorded using a Philips PW 1710 diffractometer operating with Co radiation λ=1.7903Å. Unit cells parameters of the synthesis compound have been refined by the least square method from the powder data.

RESULTS AND DISCUSSIONS

Powder X-ray analysis

X-ray powder diffractogram (figure1) reveals that the synthesized compound crystallizes in triclinic system with the space group P($\bar{1}$) and the refined unit cell parameters are: a=5.512(3)Å, b=6.929(4)Å, c=9.576(5)Å, α=105.96(1)°, β=96.29(1)° and γ= 108.80(1)° (V=324.89Å^3). The mixed compound is isotype to $Na_2PbP_2O_7$ and $Ag_2PbP_2O_7$. However, these structures consist of a tridimensional framework of $[Pb_2P_4O_{14}]^{4-}$ entities formed by the association of corner-shared PbO_5 and P_2O_7 groups; these $[Pb_2P_4O_{14}]^{4-}$ entities form ribbons parallel to the[010] direction; the ribbons are interconnected by common corners [Pb–O–P bridges] in the[100] direction and form lamina parallel to (001) plan. In both phase the monovalent cation (Na^+/Ag^+) occupies two types of site, S1 and S2. The first is localized between the $[Pb_2P_4O_{14}]^{4-}$ entities at z=1/4, the second is located between two alternating lamina at z=0, figure 2. The partial Na^+ substitution by Ag^+ cation is accompanied by a slightly increase of the volume which is due to the monovalent cation radii, r(Na^+)=1.16Å and r(Ag^+)=1.29Å[12]. Moreover, the substitution is associated by a slightly modification of all cell parameters which indicates the non selectivity of cations in both sites.

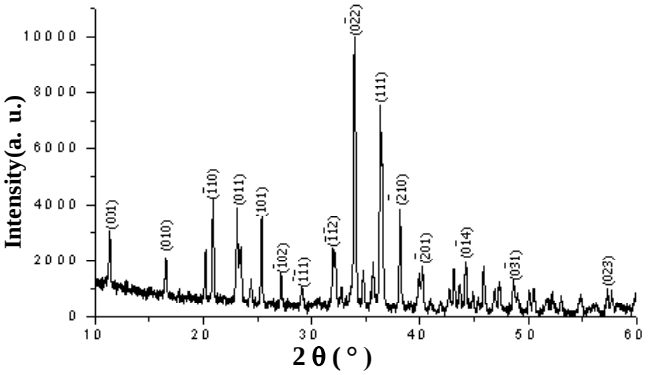

Figure 1: XRD pattern of $NaAgPbP_2O_7$.

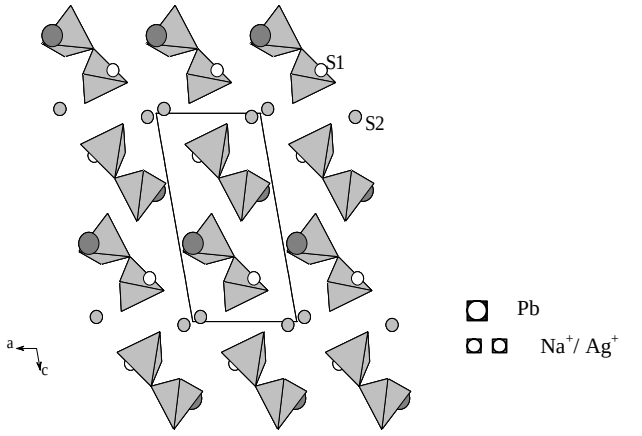

Figure 2 : Projection view of $M_2PbP_2O_7$ (M=Na, Ag) along [010] direction. The unit cell is outlined.

Impedance analysis

The impedance diagrams for $NaAgPbP_2O_7$ sample are taken in the temperature range 581-703K. The equivalent circuit allows the establishment of correlations between electrochemical parameters and characteristic impedance elements.

In the temperature range 581-609K the equivalent circuit consists of a resistance R_p (bulk resistance) and CPE_1 (capacity of the fractal interface CPE) element. The CPE_1 element accounts for the observed depression of semicircles and also the non-ideal electrode geometry. The impedance of CPE is: $Z_{CPE} = 1/Q(j\omega)^{\alpha}$. α is related to the deviation from the vertical of the line in the -Z″ versus Z′ plot. α = 1 indicates a perfect capacitance, and lower α values directly reflect the roughness of the electrode used.

For the highest temperature (T>609K), the above circuit is inadequate; the measured values disagree with the simulated one. We observe a little tail after the semicircles in the impedance spectra (fig3b inset). The straight line after the semicircle can be explained with CPE_2 corresponding to the double layer capacity of an

in-homogeneous electrode surface.

The real and the imaginary components of the whole impedance of this circuit were calculated according to the following expressions:

$$Z' = \frac{R_p^2 Q_1 \omega^{\alpha_1} \cos(\alpha_1 \pi/2) + R_p}{(1 + R_p Q_1 \omega^{\alpha_1} \cos(\alpha_1 \pi/2))^2 + (R_p Q_1 \omega^{\alpha_1} \sin(\alpha_1 \pi/2))^2} + \frac{\cos(\alpha_2 \pi/2)}{Q_2 \omega^{\alpha_2}} \quad (1)$$

$$-Z'' = \frac{R_p^2 Q_1 \omega^{\alpha_1} \sin(\alpha_1 \pi/2)}{(1 + R_p Q_1 \omega^{\alpha_1} \cos(\alpha_1 \pi/2))^2 + (R_p Q_1 \omega^{\alpha_1} \sin(\alpha_1 \pi/2))^2} + \frac{\sin(\alpha_2 \pi/2)}{Q_2 \omega^{\alpha_2}} \quad (2)$$

In figure 3 are represented Z′ and -Z″ versus frequency at 703K respectively, together with fits to the equivalent circuit of $NaAgPbP_2O_7$. The good conformity of calculated lines with experimental data indicates that the suggested equivalent circuit describes the crystal-electrolyte interface reasonably well.

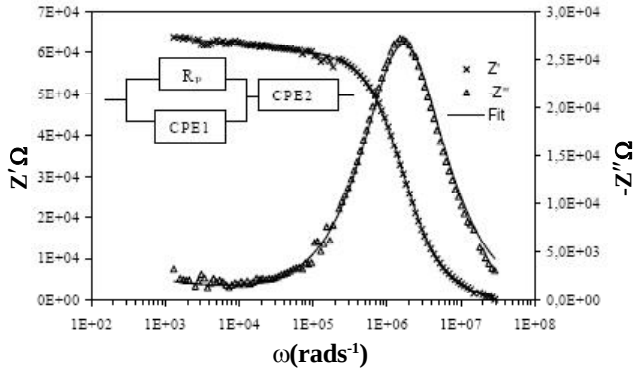

Figure 3 : Variation of Z′ and –Z″ with frequency at 703K and the equivalent circuit model of $NaAgPbP_2O_7$

Figure 4 (a) and (b) show the experimental and calculated values in (-Z″- Z′) diagram using the equivalent circuit. The depressed semicircles have their centers on a line below the real axis, which indicates departure from the ideal Debye behaviour[13].

The extract parameters for the circuit elements are summarized in table 1. It is obvious all the capacitance values Q_2 are in the range of pF. This implies that the single semicircle is from grain interiors.

The electrical conductivity $\sigma_p = e/R_pS$ plotted against temperature in an Arrhenius plot is shown in Figure 5. Following the Arrhenius law, the obtained activation energy is about 0.95(5)eV. The values of α vary in the range 0.80–1 that confirmed the weak interaction between localized sites.

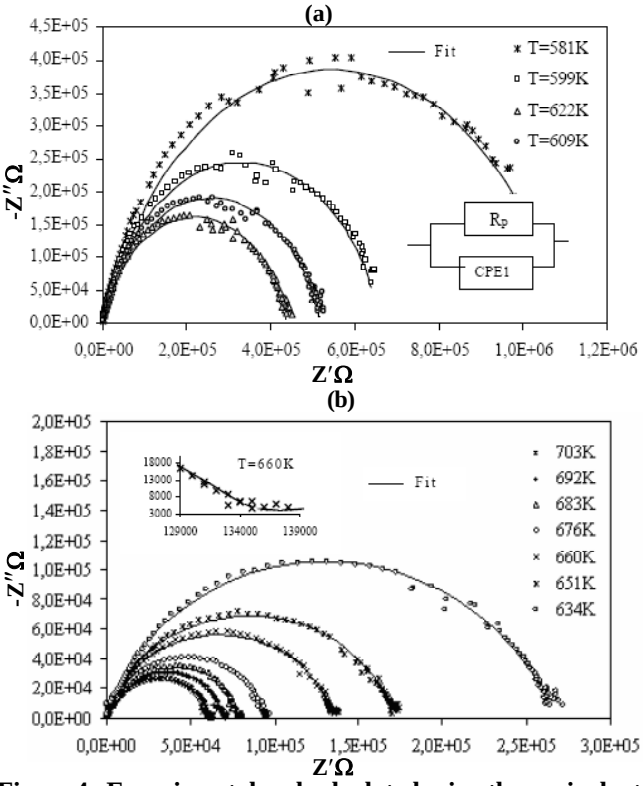

Figure 4 : Experimental and calculated using the equivalent circuit (-) semi-circle plots of Z″ vs Z′ at different temperature: (a) low temperature range, (b) high temperature range

TABLE 1 : The extract parameters for the circuit elements

T(K)	Rp(kΩ)	α_1	$Q_1(10^{-12})$	α_2	$Q_2(10^{-6})$
703	58	0.924	0.295	0.279	30
692	66	0,925	0.288	0.221	50
683	75	0,930	0.265	0.185	45
676	89	0,934	0.254	0.170	40
660	126	0,895	0.419	0.294	13
651	164	0,873	0.569	0.296	10
634	257	0.861	0.635	0.287	49
622	454	0.808	0.012		
609	539	0.809	0.012		
599	694	0.811	0.011		
581	1094	0.782	0.013		

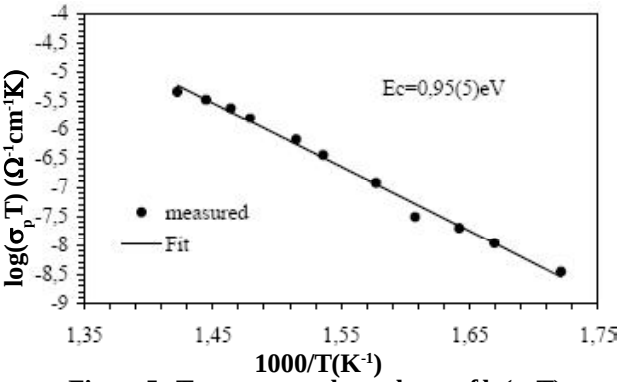

Figure 5 : Temperature dependence of $\ln(\sigma_p T)$.

Full Paper

Conductivity analysis

The conductivity of the sample has dispersion at all frequencies. It is generally analyzed using the power law[14]:

$$\sigma_{ac}(\omega) = \sigma_{dc} + A\omega^{s} \quad 0<s<1 \qquad (3)$$

Where σ_{dc} is the direct current conductivity, A is a constant for a particular temperature and s is the power exponent, it represents the degree of interaction between mobile ions and the environments surrounding them. The power law has been applied to many materials such glasses, phosphate and amorphous semiconductors[15-20].

The frequency dependence of the AC conductivity at various temperatures is determined by complex impedance analysis.

The above equation (3) has been used to fit the AC conductivity data. In the fitting procedure, A and s values have been varied simultaneously to get the best fits (Fig.6). A plot of -lnA against s indicates a linear temperature independent and structure-insensitive correlation between the values of these two parameters (Fig. 7). The values of exponent s lie in the range 0.6–1.2, the correlation motion is sub-diffusive and indicates a preference on the part of ions that has hopped away to return to where it started[21]. Jonscher[22] has shown that a non-zero s in the dispersive region of conductivity is due to the energy stored in the short range collective motion of ions. A higher s implies that large energy is stored in such collective motions. In this work, exponent s increases with increasing temperature.

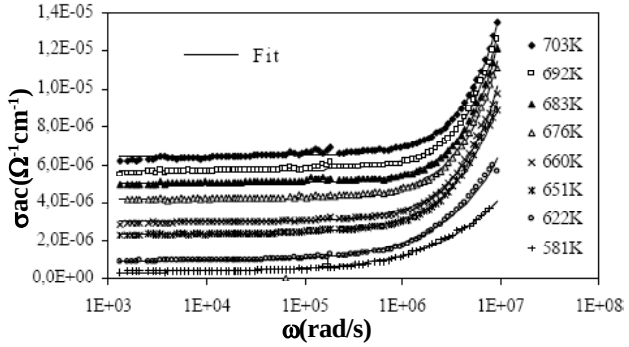

Figure 6 : Frequency dependence of AC conductivity at various temperatures

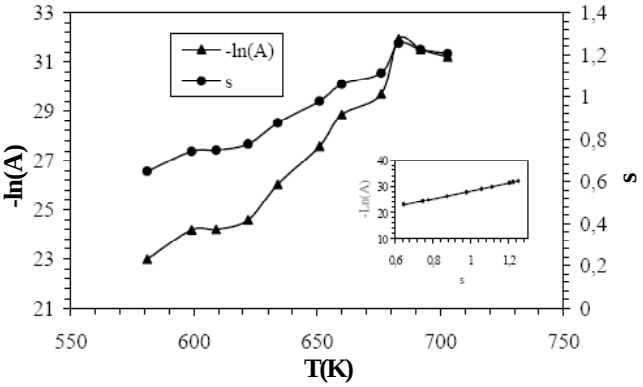

Figure 7 : Variation for universal exponents s and A as a function temperature.

DC conductivity data are plotted in Arrhenius format as $\ln(\sigma_{dc}T)$ vs 1000/T (figure 8), and show Arrhenius-type behavior described by:

$$T\sigma_{dc} = B\exp(-E_c/kT) \qquad (4)$$

Where B ($B=\sigma_0= 4.01\ 10^4\Omega^{-1}cm^{-1}K$) is the pre-exponential factor and E_C (E_C= 0.96(5)eV) is the activation energy for conduction. The transport mechanism is explained by the thermally activated hopping process between two sites separated by an energy barrier.

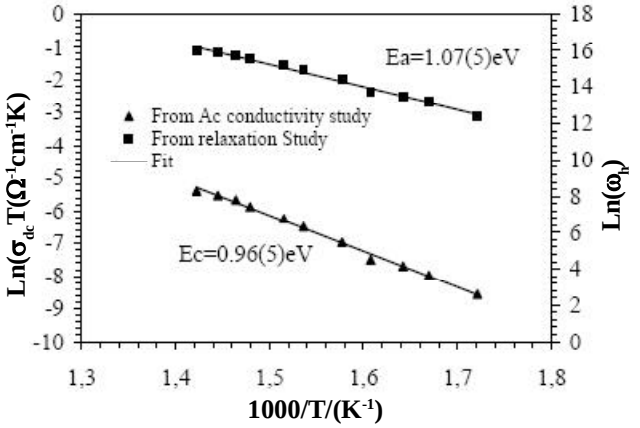

Figure 8 : Plot of DC conductivity σ_{dc} vs 1000/T

The power law can be described by the Almond–West expression[23]:

$$\sigma_{ac} = \sigma_{dc}\left[1+(\frac{\omega}{\omega_h})^{s}\right] \qquad (5)$$

Where ω_h is the hopping frequency of the charge carrier which represents the crossover frequency from dc to dispersive conductivity region at $\omega>\omega_h$. The dc conductivity σ_{dc} represents the random process in which the ion diffuse throughout the network by performing repeated hops between charge compensating sites[24]. The calculate of the hopping frequency is given by:

$$\omega_h = (\frac{\sigma_{dc}}{A})^{\frac{1}{s}} \qquad (6)$$

The variation of $\ln(\omega_h)$ with temperature is shown in figure 8, it follows Arrhenius relation with the activation energy Ea=1.07(5)eV. E_a and E_c are close, the conduction is due to the hopping mechanism.

Figure 9 shows the variation $\ln(\sigma_{ac}/\sigma_{dc})$ vs $\ln(\omega/\omega_h)$ at different temperatures. The conductivity spectra merge on a single curve, indicating that the relaxation dynamics of charge carriers in the present ceramic and β (obtained by using Kohlrausch–Williams–Watt (KWW) relaxation function) parameters of that stretched exponential function ($\varphi(t) = \exp(-t/\tau)^{\beta}$, $0 < \beta < 1$[25,26]) are independent of temperature.

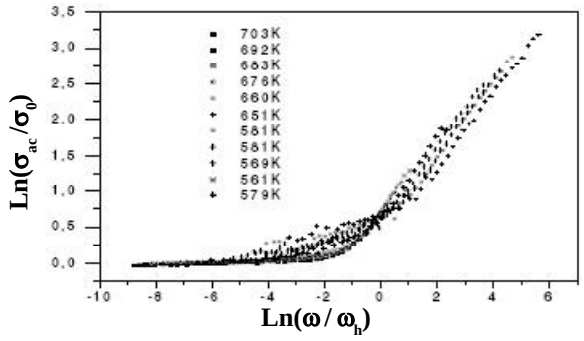

Figure 9 : Plot of log (σ_{ac}/σ_{dc}) vs. log (ω/ω_h).

Electrical data relative to $Na_2PbP_2O_7$, $Ag_2PbP_2O_7$ and $NaAgPbP_2O_7$ materials are listed in Table 2.

Compared with the parental compounds, $NaAgPbP_2O_7$ is characterised by a smaller pre-exponential factor σ_0 (Table 2).

TABLE 2 : Activation energy of ceramic $Na_2PbP_2O_7$, $Ag_2PbP_2O_7$ and $NaAgPbP_2O_7$.

Ceramic	$Na_2PbP_2O_7$[11]	$Ag_2PbP_2O_7$[10]	$NaAgPbP_2O_7$
E_c(Ev)	0.90	0.78	0.96(our study)
E_a(eV)	------	0.75	1.07(our study)
$\sigma_0(\Omega^{-1}cm^{-1}K)$	1.910^5	1.910^5	$0.4\ 10^5$(our study)

The pre-exponential factor σ_0 can be expressed as[10]:

$$\sigma_0 = (e^2 a_h^2 \nu_0/6k)\, N(T)\, \exp(S_\mu/k) \qquad (6)$$

Where a_h is the hopping distance, ν_0 is an attempt frequency to overcome the potential barrier, $N(T)$ the charge carrier concentration and S_μ is the migration entropy. In $NaAgPbP_2O_7$, the monovalent cation Na^+ or Ag^+ occupies both S1 and S2 site (fig2), it implies an increase of the disorder in material. The entropy S_μ is more important in the $NaAgPbP_2O_7$ compound. According to equation (6), we conclude that the number of charge carriers in the mixed compound is smaller than in Na and Ag phase.

The structure of $Na_2PbP_2O_7$, $Ag_2PbP_2O_7$ and $NaAgPbP_2O_7$ are isotype. The transport properties in these materials are probably due to displacements of the monovalent cation pseudo plane parallel to (001) between–S1–S2–S2–S1– conduction path[10,11].

CONCLUSION

In summary, in this work, we have synthesised the new monovalent mixed pyrophosphate $NaAgPbP_2O_7$. The compound crystallises in triclinic system ($P(\bar{1})$ space group). It is isotype to $Na_2PbP_2O_7$ and $Ag_2PbP_2O_7$ compounds. We have investigated the electrical properties of the mixed compound $NaAgPbP_2O_7$. The conductivity of the sample is analyzed at all frequencies and in temperature range 581-703K. The ac conductivity is interpreted using the power low: $\sigma(\omega) = \sigma_{dc} + A\omega^s$. The transport mechanism is explained by the thermally activated hopping process between two sites separated by an energy barrier. A comparative study with previous results $Na_2PbP_2O_7$ and $Ag_2PbP_2O_7$ shows that the conductivity in these materials is slightly higher than in the mixed compound.

REFERENCES

[1] H.G.Danielmeyer, G.Huber, W.W.Kruhler, J.F.Jesser; Appl.Phys., **2**, 335 **(1973)**.

[2] H.P.Weber, T.C.Damen, H.G.Danielmeyer, C.C.Tofield; Appl.Phys.Lett., **22**, 534 **(1973)**.

[3] J.B.Goodenough, H.Y.P.Hong, J.A.Kafalas; Appl.Phys.Lett., **11**, 203 **(1976)**.

[4] S.T.Wilson, B.M.Lok, C.A.Messina, T.R.Cannan, E.M.Flanigen; J.Am.Chem.Soc., **104**, 1146 **(1982)**.

[5] M.E.Davis, C.Saldarrige, C.Montes, J.Garces, C.Crowder; Nature, **331**, 698 **(1988)**.

[6] J.Chen, W.Pang, R.Xu; Top Catal., **9**, 93 **(1999)**.

[7] Y.Zhang, Y.Liu, S.Fu, F.Guo, Y.Qian; Bull.Chem. Soc.Jpn., **79**, 270 **(2006)**.

[8] Y.Laligant, J.Eur; Solid.State.Inorg.Chem., **29**, 239 **(1992)**.

[9] V.K.Trunov, Y.V.Oboznenko, Neorg; Mater., **27**, 1993 **(1995)**.

[10] N.Dridi, A.Boukhari, J.M.Réau, E.Arbib, E.M.Holt; Mater.Lett., **47**, 212 **(2001)**.

[11] N.Dridi, A.Boukhari, J.M.Réau, E.Arbib, E.M.Holt; Solid.State.Ionics., **127**, 141 **(2000)**.

[12] http://chemicool.com/elements/.

[13] J.R.Macdonad (Ed.); 'Impedance Spectroscopy'., Wiley; New York, **(1987)**.

[14] A.K.Jonscher; 'Dielectric relaxation in solids'., London: Chelsea Dielectrics, **(1983)**.

[15] H.Jain, J.N.Mundy; J.Non-Cryst.Solids., **91**, 315 **(1987)**.

[16] N.F.Mott, E.A.Davis; 'Electronic Progresses in Non-Crystalline Solids'., Clarendon; Oxford, **(1970)**.
[17] J.C.Dyre, T.B.Schroder; Rev.Mod.Phys., **72**, 873 **(2000)**.
[18] A.Ben.Rhaiem, N.Zouari, K.Guidara, M.Gargouri, A.Daoud; J.Alloys.Compd., **387**, 1 **(2005)**.
[19] B.Louati, M.Gargouri, K.Guidara, T.Mhiri; Journal of Physics and Chemistry of Solids., **66**, 762 **(2005)**.
[20] S.R.Elliott; Solid.State.Ionics., **27**, 131 **(1988)**.
[21] Meenakshi Pant, D.K.Kanchan, Poonam Sharma, Manish S.Jayswal; Materials Science and Engineering B., **149**, 18 **(2008)**.
[22] A.K.Jonscher; J.Mater.Sci., **16**, 2037 **(1981)**.
[23] D.P.Almond, A.R.West; Nature(Lond.)., **306**, 456 **(1983)**.
[24] M.M.Ahmed; Phys.Rev.B., **72**, 174 **(2005)**.
[25] K.L.Ngai, S.W.Martin; Phys.Rev., **B40**, 10550 **(1989)**.
[26] F.S.Howell, R.A.Bose, P.B.Macedo, C.T.Moynihan; J.Phys.Chem., **78**, 639 **(1974)**.